Long title: A revised understanding of *Tribolium* morphogenesis further reconciles short and long germ development

Short title: A major revision to our understanding of short germ embryogenesis

Author: Matthew A. Benton

Author affiliation: Department of Zoology, University of Cologne, Cologne, NRW, Germany

Corresponding author: Matthew A. Benton, matthewabenton@gmail.com

Abstract

In *Drosophila melanogaster*, the germband forms directly on the egg surface and solely consists of embryonic tissue (termed long germ development). In contrast, most insect embryos undergo a complicated set of tissue rearrangements to generate a condensed, bi-layered germband (termed short/intermediate germ development). The ventral side of the germband is embryonic, while the dorsal side is thought to be an extraembryonic tissue called the amnion. While this tissue organisation has been accepted for decades, and has been widely reported in insects, its accuracy has not been directly tested in any species. Using live cell tracking and differential cell labelling in the short germ beetle *Tribolium castaneum*, I show that most of the cells previously thought to be amnion actually give rise to large parts of the embryo. This process occurs via the dorsal-to-ventral flow of cells and contributes to germband extension. In addition, I show that true 'amnion' cells in *Tribolium* originate from a small region of the blastoderm. Together, my findings show that development in the short germ embryos of *Tribolium* and the long germ embryos of *Drosophila* is more similar than previously proposed. Dorsal-to-ventral cell flow also occurs in *Drosophila* during germband extension, and I argue that the flow is driven by a conserved set of underlying morphogenetic events in both species. Furthermore, the revised *Tribolium* fatemap that I present is far more similar to that of *Drosophila* than the classic *Tribolium* fatemap. Lastly, my findings show that there is no qualitative difference between the structures of the blastoderm and the short/intermediate germ germband. As such, the same tissue patterning mechanisms could function continuously throughout the cellularised blastoderm and germband stages, and easily shift between them over evolutionary time.

Introduction

Insects are the most speciose phylum of animals and display remarkable diversity in adult morphology (1). Insect embryo development is also very diverse, particularly in the stages leading to the formation of the elongated, segmented embryo (called the germband) (2). The molecular and morphogenetic basis of this process is best understood in the fly *Drosophila melanogaster*. In this species, a predominantly hierarchical chain of patterning events specifies nearly all segments more-or-less simultaneously at the syncytial blastoderm stage (3). Cellularisation takes place near the end of this process, after which point morphogenetic events such as germband extension (GBE) occur (see Fig 1 for schematic summary). The *Drosophila* mode of development is termed long germ development and is fairly representative of most true flies (4). In contrast, the vast majority of insects undergo short or intermediate germ development, meaning that only a handful of segments are specified at the blastoderm stage and the remaining segments are specified sequentially as the germband elongates (5).

Short germ development has been best studied in the beetle *Tribolium castaneum,* and recent research has shown that development in this species is more similar to *Drosophila* than previously thought. For example, while previous molecular studies have suggested that *Tribolium* segment specification occurs in a qualitatively different way to *Drosophila* (6,7), recent detailed analyses have shown that a relatively conserved patterning network may underlie segment specification in both species (8–10).

The morphogenetic events occurring during GBE are also more conserved than previously thought. In *Drosophila*, GBE is predominantly driven by the mediolateral intercalation of ectodermal cells (i.e. convergent extension), although cell deformation along

61 the anterior-posterior (AP) axis and cell divisions are also involved (11–16). In contrast to
62 this, *Tribolium* germband elongation was previously thought to be driven by the so-called
63 'growth zone' at the posterior of the germband (17). Now, however, it is clear that *Tribolium*
64 germband elongation is also predominantly driven by mediolateral cell intercalation (see Fig
65 1 for schematic summary of *Tribolium* development) (7,18,19). Furthermore, in both
66 *Tribolium* and *Drosophila*, this intercalation requires the striped expression of a specific
67 group of Toll genes (so-called Long Toll/Loto class genes) (20,21).

68 It is highly likely that germband elongation mediated by cell intercalation is
69 homologous in these two species, and probably in other arthropods, as well (21). As such, I
70 will hereafter refer to *Tribolium* 'germband elongation' as 'germband extension'/GBE,
71 unifying the *Drosophila*/*Tribolium* terminology. In addition, as there is no evidence for a
72 qualitatively different 'growth zone' in *Tribolium* (i.e. a specialised zone of volumetric
73 growth), I will refer to the posterior unsegmented region as the 'segment addition zone'
74 (8,23,24).

75 Despite the similarities described above, substantial differences in the embryonic
76 fatemaps of these species exist (Fig 1). In *Drosophila*, almost the entire blastoderm is fated
77 as embryonic tissue, and only a small dorsal region is fated as extraembryonic tissue (termed
78 the amnioserosa) (22). In contrast, in *Tribolium*, roughly the anterior third of the blastoderm
79 gives rise to an extraembryonic tissue called the serosa (25). Of the remaining blastoderm, a
80 large dorsal region is thought to give rise to a second extraembryonic tissue called the
81 amnion, with only the remaining ventral tissue giving rise to the embryo itself (26–28). Like
82 the amnioserosa, the serosa and the amnion are proposed to support the embryo during
83 development, but are thought to degenerate prior to hatching and not contribute to any
84 larval or adult structures (29,30).

85 *Drosophila* and *Tribolium* also exhibit dramatic differences in the morphogenetic
86 events occurring during early development (Fig 1). When GBE occurs in *Drosophila*, the
87 germband stays at the surface of the egg and the amnioserosa largely remains in place. In
88 *Tribolium*, on the other hand, germband extension begins with a complicated process called
89 embryo formation (see Fig 1; for a detailed description see (18,31)). During this process, the
90 presumptive embryonic ectoderm condenses towards the ventral side of the egg via both
91 mediolateral cell intercalation and a cuboidal-to-columnar cell shape transition.
92 Simultaneously, epithelial folding and tissue involution occurs, causing the presumptive
93 amnion to fold over the embryo to form the multi-layered germband. During these
94 movements, the serosa cells undergo a cuboidal-to-squamous transition and spread over the
95 entire egg surface.
96 The differences in fatemap and tissue folding described above show that both
97 fatemap shifts and reductions in early morphogenetic events have contributed to the
98 evolution of the long germ mode of development. Understanding how these differences
99 evolved is integral to understanding the short-to-long germ transition, but in order to study
100 how this occurred, we first need to understand how these tissues develop in each species.
101 The form and function of the *Tribolium* serosa has been analysed in several studies
102 (25,32,33), and comparative research in several fly species has revealed how the
103 loss/reduction of the serosa in flies may have occurred (reviewed in (29)). The amnion, on
104 the other hand, has proven harder to analyse, and the precise embryo/amnion boundary at
105 the blastoderm stage is unknown. However, a clear boundary between embryo and amnion
106 has been proposed to exist at the germband stage (Fig 1) (26). Cells in the ventral half of the
107 germband are thought to give rise to all embryonic structures, while cells in the dorsal half of
108 the germband are thought to form the amnion (28,34,35). This germband structure has been

109 described in many insects over the past century and is proposed to represent the core
110 conserved structure of short/intermediate germ embryos (reviewed in (2,36,37)). However,
111 the proposed boundary between cells fated to become embryo and those fated to become
112 amnion has not been directly tested.

113 I here set out to investigate the development of the presumptive amnion in *Tribolium*
114 using a combination of fluorescent live imaging and fate mapping techniques. To my great
115 surprise, I find that the majority of the cells previously described as 'amnion' actually form
116 large parts of the embryo proper. Using fate-mapping experiments, I show that true
117 'amnion' cells originate from a very small domain of the blastoderm, just as the *Drosophila*
118 amnioserosa cells do. I also show that the movement of cells from the 'amnion' side of the
119 germband to the 'embryo' side of the germband occurs via the large scale flow of the
120 ectodermal epithelium. Lastly, I describe the underlying causes of this flow, and show how
121 this tissue movement is likely homologous to the dorsal-to-ventral tissue flow that occurs
122 during *Drosophila* GBE.

123 This discovery forces a major shift in our view of development in *Tribolium* (and of
124 short/intermediate germ insects in general) and demonstrates that there is no qualitative
125 difference in germband tissue structure between *Tribolium* and *Drosophila*. Furthermore,
126 this discovery has significant consequences for how we must study short/intermediate germ
127 development going forward, as what was previously thought to be amnion (but is actually a
128 large region of the embryo) is routinely discarded or ignored during sample preparation.

129

130

131

132 **Results**

133 **Live cell tracking reveals movement of 'amnion' cells into the embryo**

134 To examine the development of the *Tribolium* presumptive amnion in detail, I carried out
135 high resolution live imaging of embryos transiently labelled (18) with a fluorescent histone
136 marker (H2B-venus) to label nuclei. My goal was to track presumptive amnion cells from the
137 blastoderm stage onwards. However, it was not possible to accurately track the majority of
138 cells throughout embryo condensation and GBE, due to the extensive morphogenetic
139 rearrangements that take place during this process. Instead, I focused on the stage
140 immediately following condensation, when the multi-layered germband has formed, and the
141 embryonic region where the presumptive amnion is closest to the surface of the egg.
142 Specifically, I tracked over 200 presumptive amnion cells in the central region of the embryo
143 from the closure of the serosa window until after the formation of the thoracic segments
144 (over 11 hours of development; Fig 2 Supplemental Movie 2). As previously described (18),
145 the germband and yolk exhibit pulsatile movements during this period, as well as rotating
146 within the serosa (Supplemental Movie 1).

147 The presumptive amnion initially consisted of many tightly packed cells that became
148 increasingly spread out during GBE (Supplemental Movie 2, Fig 2(A-C)). However, rather than
149 remaining restricted to the 'amnion territory', many of the tracked cells moved around the
150 edge of the germband in to the 'embryo territory'. Differential labelling of tracked cells
151 clearly showed that these cells that moved around the germband edge became part of the
152 embryo proper (Supplemental Movie 2 and Fig 2(A-C)). The cells that joined the 'embryo
153 territory' became tightly packed, continued to divide, and formed embryonic structures
154 (Supplemental Movie 3 and Fig 2(D-F)). In contrast, cells that remained in the 'amnion
155 territory' became squamous and stopped dividing. The nuclei of these latter cells became
156 enlarged (Supplemental Movie 3 and Fig 2(D-F)), suggesting that they underwent

157 endoreplication to become polyploid, as seen in the *Tribolium* serosa and in the *Drosophila*
158 amnioserosa (22,27). In addition, several germband nuclei underwent apoptosis
159 (Supplemental Movie 3) as has been described in fixed embryos (38). These results show
160 that many of the cells previously thought to be extraembryonic amnion give rise to
161 embryonic structures. As such, it is not accurate for the entire epithelium to be called
162 'amnion' and I will instead refer to it as the 'dorsal epithelium' as this region is made up of
163 dorsal/dorsolateral ectoderm.
164
165 **Differential cell labelling confirms widespread dorsal-to-ventral cell movement**
166 My next question was whether the movement of cells from the dorsal epithelium to the
167 ventral epithelium occurs throughout the AP axis or is just limited to the thoracic region. The
168 extensive movements of the germband made it difficult to track individual cells accurately at
169 the anterior and posterior poles. To overcome this problem, I combined differential cell
170 labelling with long term fluorescent live imaging to follow small groups of nuclei throughout
171 development. Specifically, I microinjected mRNA encoding a nuclear-localised
172 photoconvertable fluorescent protein (NLS-tdEos) into pre-blastoderm embryos to uniformly
173 label all nuclei, then photoconverted a small patch of nuclei at different positions along the
174 AP axis at the final uniform blastoderm stage. I then performed long term confocal live
175 imaging of both the unconverted and photoconverted forms of the fluorescent protein
176 throughout the period of GBE (or longer). Unlike that of *Drosophila*, the *Tribolium* egg shell
177 does not show any dorsoventral (DV) polarity, and I was therefore unable to specifically
178 target particular locations along the DV axis. Instead, I opted for a brute-force approach and
179 performed the photoconversion experiment for 50-150 embryos at each AP position (75%
180 egg length [EL] from the posterior pole, 50% EL, 25% EL, and close to the posterior pole), and

181 then used the subsequent live imaging to determine the DV position of the photoconverted
182 cells. Using a new live imaging set up (see Materials and Methods), I obtained the same
183 range of hatching rates as I typically obtain for other microinjection experiments
184 (approximately 80%, REF), even after continuous confocal live imaging for almost the
185 entirety of *Tribolium* embryonic development (3.5 days; Supplemental Movie 4). Both
186 unconverted and photoconverted protein persisted throughout germband extension and
187 retraction, although fluorescent signal faded over time. I have included various examples
188 from this data set in Supplemental Figures 1-3. In addition, I have made the raw confocal
189 data for a large number of timelapses available online (>300 embryos, >700 GB of data,
190 [upload in progress at time of submission]) for the benefit of the community. This data will
191 likely prove valuable for a wide range of research projects.

192 During my live imaging, ectodermal cell clones became elongated along the AP axis
193 over time, as previously reported in a *Tribolium* study that used a non-live imaging cell clone
194 method (19). However, Nakamoto and colleagues stated that "labelled ectodermal cells …
195 rarely mix with unlabelled cells" even as clones became greatly elongated. In contrast, I
196 frequently observed non-converted nuclei in the midst of labelled nuclei (Fig 3(A-F),
197 Supplemental Figures 1-3), confirming that extensive mediolateral cell intercalation occurs
198 throughout GBE. This difference in clone behaviour between the two approaches may be
199 due to differences in the size of the initial group of photoconverted cells, or in the resolution
200 of the subsequent imaging.

201 When I examined clones initially located in the dorsal epithelium, I found that
202 movement of cells from the dorsal epithelium to the ventral epithelium occurred throughout
203 the posterior of the embryo during GBE (Fig 3(A-F), Supplemental Movie 5). I also observed
204 the same movements at the anterior of the germband (Fig 3(G-J)), although I have focused

205 my analysis on the middle and posterior parts of the embryo. Together with the cell tracking
206 data, these results show that most of what was previously thought to be 'amnion' is in fact
207 embryonic tissue, and that cells move from the dorsal epithelium to the ventral epithelium
208 throughout the germband (summarised in Fig 3(K,L))

209 Support for these findings also comes from comparing the expression pattern of the
210 transcription factor Caudal in both *Tribolium* and *Drosophila*. In both species, this gene is
211 initially expressed in a broad posterior domain that then retracts along the AP axis (39,40). In
212 *Drosophila,* expression persists for longer in dorsal tissue than ventral tissue (9). Similar
213 dorsoventral dynamics, although not previously remarked upon, are also evident in
214 *Tribolium*; *Tc-cad* expression does indeed persist longer in the dorsal epithelium than in the
215 ventral epithelium (Supplemental Fig 4).

216

217 ***Tribolium serpent* may mark true 'amnion'**

218 As described earlier, cells that remained in the dorsal epithelium became squamous, and this
219 cell shape change occurred progressively along the AP axis (Fig 4(A)). This change in cell
220 shape may be a sign of maturation of true 'amnion'. While characterising cell fate markers, I
221 found that the *Tribolium* ortholog of the GATA factor *serpent* (*Tc-srp*) exhibited spatial and
222 temporal expression dynamics that were very similar to those of the potential 'amnion' (Fig
223 4(B), Supplemental Fig 5). At the end of GBE, all but the posterior-most cells of the dorsal
224 epithelium were squamous (data not shown) and *Tc-srp* seemed to be expressed in dorsal
225 epithelium cells along nearly the full length of the germband (Supplemental Fig 5(I_2)).
226 However, this latter finding was difficult to confirm as most of the dorsal epithelium is lost
227 during embryo fixation at this embryonic stage (presumably due to the fragility of the
228 tissue). I also found *Tc-srp* to be expressed in several other domains, including in the

229 presumptive endoderm (Supplemental Fig 5). In *Drosophila*, *serpent* is also expressed in
230 extraembryonic tissue (the amnioserosa) (41–44), and, therefore, *Tc-srp* may mark 'true'
231 extraembryonic amnion. However, future work is required to confirm whether this putative
232 amnion degenerates prior to hatching (as is required to be defined as extraembryonic). For
233 simplicity, I will refer to this tissue as 'amnion' for the remainder of this text.
234
235 **A revised *Tribolium* fatemap**
236 To determine which blastoderm cells give rise to the amnion, I analysed 85 embryos in which
237 the dorsal and dorsolateral blastoderm cells were labelled by NLStdEos photoconversion as
238 described above. I found that amnion cells arose from a very small domain of dorsal-most
239 cells (that tapers from its anterior to posterior extent) and from a narrow strip of cells
240 between the presumptive embryo and presumptive serosa (summarised in Fig 5 and
241 Supplemental Fig 6). At 50% EL, only approximately the 6 dorsal-most cells (approximately
242 8% of the circumference of the blastoderm) gave rise to all amnion cells stretching from one
243 side of the thorax to the other (Fig 4(C), Supplemental Fig 1). Nearer to the posterior of the
244 blastoderm (25% EL), even fewer cells gave rise to amnion (approximately 3 of the most
245 dorsal cells; approximately 6% of the circumference; Fig 4(D), Supplemental Fig 2). The
246 posterior limit of the amnion was difficult to define, as although some cells from
247 approximately 5-10% EL appeared to become amnion (Fig 4(E)), these cells condensed
248 posteriorly towards the hindgut during germband retraction, and might have contributed to
249 the hindgut tissue (Supplemental Fig 3, Supplemental movie 6). I was unable to
250 unambiguously determine the fate of these cells. At the anterior of the embryo, I found that
251 a narrow strip of 1-2 cells between the presumptive embryo and presumptive serosa also
252 gave rise to amnion (Fig 3(G-J)). Substantial additional work is required to define a complete

253 blastoderm fatemap for *Tribolium*, however, my findings show that the 'amnion' domain is
254 drastically smaller than previously proposed.
255
256
257 ## Discussion
258 In this article, I have shown that the majority of cells that were previously thought to be
259 extraembryonic amnion actually give rise to embryonic tissue. The movement of cells from
260 the dorsal side of the germband to the ventral side was visible in live cell tracking and
261 differential cell labelling experiments. My results also show that the true amnion region
262 appears to differentiate progressively along the AP axis during GBE, as shown by differences
263 in cell behaviour and the expression of the gene *Tc-srp*. Lastly, the cells that give rise to this
264 presumptive amnion predominantly originate from a small domain on the dorsal side of the
265 blastoderm.
266
267 **A revised understanding of the short germ embryo**
268 The revision to the blastoderm fatemap is essentially a quantitative shift in our
269 understanding of where cell fate boundaries lie along the DV axis. In the revised *Tribolium*
270 blastoderm fatemap (Fig 5, Supplemental Fig 6), the proportion of the blastoderm that gives
271 rise to the presumptive amnion is much smaller than previously thought. The presumptive
272 amnion domain is, therefore, remarkably similar in size to the amnioserosa domain of the
273 *Drosophila* blastoderm fatemap (22). However, it is important to recognize that fatemaps
274 such as those presented here show a static picture of a dynamic process. There is no
275 evidence that the presumptive amnion is specified at the blastoderm stage in *Tribolium*.
276 Instead, the progressive changes in cell shape and *Tc-srp* expression in the dorsal epithelium

277 of the germband suggest that the amnion is specified progressively along the AP axis during
278 GBE. Progressive specification of DV cell fates during GBE fits with previous hypotheses
279 (34,45), and analysis of how this process occurs represents an exciting avenue of future
280 research (possible mechanisms are discussed more later).

281 In contrast to the fatemap revision, the observation that cells move from the dorsal
282 half of the germband to the ventral half of the germband represents a qualitative shift in our
283 understanding of development in short/intermediate germ insects. In the classic model of
284 short/intermediate germ development, the germband was thought of as a more-or-less flat
285 sheet of ectodermal cells (with mesoderm underneath) covered dorsally by the
286 extraembryonic amnion. Because of this, the entire dorsal epithelium is routinely removed
287 during embryo preparation, or not included in descriptions of gene expression patterns and
288 embryonic phenotypes. Based on the new data presented here, it is obvious that we have
289 been discarding or ignoring large parts of the embryo. Furthermore, the movement of cells
290 from the dorsal epithelium into the ventral epithelium must be contributing to GBE, and is,
291 therefore, a key aspect of the extension and overall development of the germband that has
292 thus far been missed.

293 The revised model of the germband does present some technical challenges for
294 future work on short/intermediate germ embryo. The flattened geometry of the germband
295 makes it difficult to image both the dorsal and ventral epithelium using bright-field
296 microscopy approaches. However, this problem can be overcome either by using
297 fluorescence based techniques and confocal microscopy or by mechanical sectioning of the
298 germband. Both approaches have been shown to work well in *Tribolium* (for example see
299 (7,46) and results in this manuscript). In the rest of this article, I discuss why the revised
300 fatemap and cell flow accord well with what we know about *Tribolium* development, and

301 outline the implications of this discovery on our understanding of the evolution of insect
302 development.
303
304 **The cellular and molecular causes of tissue flow unify the blastoderm and the germband**
305 The revised model of the *Tribolium* germband reconciles the blastoderm and germband
306 stages. The ectoderm of the germband is a continuous epithelium, which means that the
307 movement of cells from the dorsal epithelium to the ventral epithelium occurs as a tissue
308 level 'flow'. Such dorsal-to-ventral tissue flow also occurs during embryo condensation in
309 *Tribolium* (18), and I propose that the flow is caused by largely the same morphogenetic
310 processes at both stages. The evidence for this hypothesis is summarised here, but for an
311 extended discussion see Appendix section 1.
312 Three morphogenetic processes contribute to dorsal-to-ventral cell flow in *Tribolium*,
313 and at least two of the three occur at both the blastoderm and germband stages. First,
314 mediolateral cell intercalation occurs at both stages and causes tissue-wide convergence
315 (along the DV axis) and extension (along the AP axis). This process requires two *Toll* genes
316 that are expressed in rings around the entire blastoderm and germband epithelium (21).
317 Second, tissue specific cell shape changes occur at both stages such that ventral/lateral cells
318 become columnar and dorsal/dorsolateral cells become thinner (during condensation
319 (Supplemental Fig 7)) or squamous (during GBE). The tissue level effect of these changes is
320 contraction of the ventral/lateral tissue and spreading of the dorsal tissue. The flattening of
321 dorsal/dorsolateral cells is likely regulated by BMP signalling, as not only does BMP activity
322 correlate with the cell shape changes (see Appendix section 1), but functional disruption of
323 BMP signalling components leads to uniform cell shape changes along the DV axis (28,47). A
324 third major morphogenetic event is gastrulation of the mesoderm. This occurs along the

325 ventral midline, and as gastrulation occurs, the ectoderm moves ventrally to seal the gap left
326 in the epithelium (46). At the stage when a complete germband has formed, gastrulation is
327 complete along most of the embryo. However, current data suggests mesoderm gastrulation
328 may be ongoing in the segment addition zone (46). If true, the ongoing invagination would
329 contribute to tissue flow in this region.

330 It is important to note that while each of the events described here is involved in the
331 dorsal-to-ventral tissue flow, no single event is absolutely required for it. In the absence of
332 cell intercalation, embryo condensation and thinning of dorsal/dorsolateral ectoderm still
333 takes place yielding abnormally wide and short germbands (21). In the absence of tissue
334 specific cell shape changes, condensation occurs in a more radially symmetrical manner
335 yielding a tube-shaped germband that undergoes segment specification and convergent
336 extension (28,47). Finally, both condensation and GBE are only mildly affected in the
337 absence of mesoderm specification (48). This functional independence comes from each of
338 the three process being specified by different pathways (intercalation via segment
339 specification, dorsal thinning via dorsal tissue specification, and gastrulation via ventral
340 tissue specification). There may be further, as yet undiscovered morphogenetic events that
341 also contribute to the dorsal-to-ventral tissue flow.

342

343 **Reconciling long and short germ development**

344 I propose that the dorsal-to-ventral tissue flow occurring during embryo condensation and
345 GBE in *Tribolium* is homologous to the dorsal-to-ventral tissue flow that occurs during
346 gastrulation and GBE in *Drosophila* (Fig 1). This conclusion is based on the flow being driven
347 by a conserved set of morphogenetic events.

348 As described above, tissue flow in *Tribolium* is caused by (1) mediolateral cell
349 intercalation, (2) tissue specific cell shape changes along the DV axis, and (3) gastrulation at
350 the ventral side of the embryo. Equivalent processes are all observed in *Drosophila* as well.
351 In *Drosophila*, *Toll*-mediated mediolateral cell intercalation causes the tissue wide
352 convergence (along the DV axis) and extension (along the AP axis) of the ectoderm during
353 GBE (20). As in *Tribolium*, the periodic expression of the *Toll* genes is driven by the pair-rule
354 genes. Conservation at the level of tissue identity, morphogenetic process, and molecular
355 control strongly suggest *Toll*-mediated cell intercalation to be homologous.
356 Cell shape changes are harder to compare between these species, as unlike most
357 insects, cellularisation in *Drosophila* leads to the direct formation of columnar cells (22,49).
358 However, tissue specific cell shape changes along the DV axis do occur and are dependent on
359 BMP signalling ((50,51); for a detailed description see Appendix section 2). While the
360 intracellular effectors of these cell shape changes are unknown, the dorsal patterning
361 function of BMP signalling is homologous in *Drosophila* and *Tribolium*, and many dorsal cell
362 specification genes are conserved between these two species.
363 Last, *Drosophila* mesoderm gastrulation also occurs along the ventral midline and it
364 causes lateral/dorsolateral ectoderm to move ventrally (50). As above, the intracellular
365 effectors of *Tribolium* mesoderm gastrulation are unknown, but the upstream patterning
366 events and the tissue specification genes are highly conserved (34,48). Furthermore,
367 gastrulation of mesoderm at the ventral region is widely conserved within the insects, and is
368 undoubtedly a homologous process in each species (52).
369 The conservation of the tissue-level flow and the underlying processes shows that
370 development in *Drosophila* and *Tribolium*, which are themselves models for long and short
371 germ development respectively, are far more similar than previously thought. This similarity

372 is further emphasised when the *Tribolium* germband is represented as a cylinder rather than
373 its normal *in vivo* flattened shape (Fig 6). This finding helps explain how the long germ mode
374 of development has evolved independently many times, as it takes fewer evolutionary
375 'steps' to go from one form to another than previously thought.

376 While I have focused on *Tribolium* and *Drosophila* here, evidence exists that my new
377 findings in *Tribolium* also apply to other short/intermediate germ insects. For example, in
378 the intermediate germ bug *Oncopeltus fasciatus*, the dorsal epithelium of the germband
379 initially consists of a thick epithelium that then progressively becomes squamous late during
380 GBE ((53) and data not shown). These tissue specific cell shape changes are likely the same
381 as those occurring during *Tribolium* GBE. Furthermore, *Oncopeltus* pair-rule genes, Loto *Toll*
382 genes and even segment polarity genes are expressed in rings around the entire germband
383 prior to thinning of the dorsal epithelium (shown but not described in (21,54,55)). The
384 expression of these genes in the dorsal epithelium provides additional evidence that much of
385 the *Oncopeltus* dorsal epithelium is made up of embryonic tissue. Future analyses of the
386 molecular and morphogenetic drivers of GBE need to analyse the entire germband, rather
387 than focusing on the ventral half.

388

389 **The *Drosophila* posterior gut fold may represent an evolutionary remnant of short germ**
390 **development**

391 Despite the deep conservation in morphogenetic events described above, a very obvious
392 difference exists between the germbands of *Drosophila* and *Tribolium*. While the *Drosophila*
393 germband develops mostly on the egg surface with the apical side of the epithelium facing
394 outwards, the epithelium of the *Tribolium* germband folds onto itself such that the apical
395 side faces inwards (Fig 1). The last common ancestor of *Tribolium* and *Drosophila* almost

396 certainly exhibited short/intermediate germ development (56), which would include the
397 formation of a bi-layered germband like that of *Tribolium*. As such, in the lineage leading to
398 *Drosophila*, the epithelial folding that previously generated the bi-layered germband must
399 have become heavily reduced during evolution.

400 I propose that remnants of the folding seen in *Tribolium* still exists in *Drosophila*
401 today, in what is now termed the "posterior gut fold". The epithelial folding that causes the
402 formation of the bi-layered germband of *Tribolium* initiates with a deep infolding of tissue at
403 the posterior of the embryo (classically termed the posterior amniotic fold) (18,27).
404 Epithelial infolding also occurs at the posterior of the *Drosophila* blastoderm during posterior
405 gut formation (57), and the similarities between these folds have been pointed out before
406 (27). However, the evolutionary relationship of these two structures has been unclear due to
407 the belief that the dorsal half of the fold in *Tribolium* gave rise to the amnion. Now, with the
408 revised fatemap, it is clear that these folds form from the same region of the embryo.
409 Therefore, I propose that the epithelial fold that forms during posterior gut formation in
410 *Drosophila* is homologous to the posterior epithelial fold that forms during embryo
411 condensation in *Tribolium*. This hypothesis is supported by two pieces of molecular data.
412 First, a recent report found that a gene essential for hindgut development (the *Tribolium*
413 ortholog of *senseless*) is already expressed at the posterior pole of the *Tribolium* embryo at
414 the blastoderm stage (58). Second, the *Tribolium* posterior fold is controlled at the
415 morphogenetic level by the Fog signalling pathway, just like it is in *Drosophila* (Frey et al.
416 manuscript in preparation).

417 Due to this revised evolutionary relationship and the new *Tribolium* fatemap, I
418 propose that the posterior fold in *Tribolium* be renamed from 'posterior amniotic fold' to
419 'posterior fold'.

420

421 **New insights in tissue patterning**

422 While I have predominantly focused on morphogenetic events in this manuscript, the
423 revised model of short germ embryo development also has impacts for how we understand
424 tissue patterning to occur in *Tribolium*. Here, I present one example of this, but for
425 descriptions of pair-rule gene expression, posterior terminal gene expression, and of how DV
426 patterning may be occurring in the germband, see Appendix section 3.

427 Segment polarity genes are expressed in a single stripe in each segment, extending
428 from near the ventral midline of the embryo to the lateral edge of the germband (59–61).
429 Under the classic model, these domains appear to be static. However, the revised model
430 shows that cells at the lateral edges of the germband move ventrally as cells from the dorsal
431 epithelium move around the edges of the germband. This means that for each stripe of a
432 segment polarity gene to 'stay' at the edge of the germband, cells at the correct AP location
433 must activate segment polarity gene expression when they move from the dorsal epithelium
434 to the ventral. This can be thought of like Lewis Carroll's Red Queen's race, where "it takes
435 all the running you can do, to keep in the same place" (62). These dynamics mean that each
436 expression domain spreads from ventral-to-dorsal across the ectoderm, but that this occurs
437 simultaneously with the dorsal-to-ventral flow of tissue. A similar ventral-to-dorsal activation
438 of segment polarity gene expression can be seen in the *Drosophila* ectoderm (Supplemental
439 Fig 8), indicating that the DV position of expression is controlled by a conserved upstream
440 mechanism.

441 While I have only described a handful of examples in this manuscript, other genes are
442 likely to have important expression domains in both the ventral and dorsal epithelia of the

443 germband. Accurately characterising these domains is necessary for understanding how
444 these genes function in *Tribolium* and for elucidating how their functions may have evolved.
445
446 **Conclusions**
447 The deep conservation of morphogenetic events that I am proposing here may seem
448 unlikely, but I would argue that such conservation should have been expected from the
449 beginning. The vast majority of morphogenetic events are controlled by upstream patterning
450 networks. As such, morphogenesis can be viewed as a physical readout of such networks.
451 Decades of research has shown that many of the key patterning genes that function during
452 germband formation and extension in *Drosophila* have conserved roles in *Tribolium* and
453 other insects. As such, without evidence to the contrary, conservation of the cellular events
454 driven by these patterning genes makes perfect sense.
455
456
457 **Materials and methods**
458 *Tribolium* animal husbandry, egg collection, and RNA *in situ* hybridisation was performed as
459 previously described (21). The *Tc-srp* ortholog was previously described (63) and was cloned
460 into pGEM-t (Promega Reference A1360) with primers TCCCGCTGCTTTGATCTAGT and
461 TGCGATGACTGTGACGTGTA. The *Tc-cad* ortholog was as previously used (18).
462 The *H2B-ven* fusion was created by fusing the *D. melanogaster* histone *H2B* coding
463 sequence (without the stop codon) from the published H2B-RFP (18) to the *venus*
464 fluorescent protein (64) and cloning into the pSP64 Poly(A) (Promega Reference P1241)
465 expression vector. The *NLS-tdEos* fusion was kindly provided by Matthias Pechmann.
466 Additional details and both plasmids are available upon request to M. Pechmann or myself.

467 Capped mRNA synthesis was performed as previously described (18). *H2B-ven* capped mRNA
468 was injected at 1 µg/µL, *NLS-tdEos* capped mRNA was injected at 2-3 µg/µL.
469 Embryo microinjection was performed as previously described (18), with the
470 following changes. Up to 100 dechorionated embryos were mounted on a rectangular
471 coverslip (24 mm by 50 mm) that rested on a microscope slide. Water was allowed to dry off
472 the embryos before they were covered in Voltalef 10S halocarbon oil and injected as usual.
473 The coverslip (still resting on the slide) was then placed in a petri-dish (92 mm) containing a
474 base layer of 1% agarose (dissolved in water) and placed at 30-32°C until the embryos were
475 at the appropriate stage for imaging. The coverslip was then removed from the slide,
476 inverted (so that embryos were face down), and quickly but gently placed on a lumox dish
477 (50 mm; Sarstedt Reference 94.6077.410) that was sitting upside down. The corners of the
478 coverslip rested on the raised plastic lip of the dish such that the membrane and embryos
479 were close to each other but not touching. To ensure lateral stability of the coverslip during
480 the timelapse recording, approximately 5-10 µL of heptane glue (made by soaking parcel
481 tape in heptane) was placed at each corner. Additional Voltalef 10S halocarbon oil was then
482 added to fill any remaining space between the coverslip and the oxygen permeable
483 membrane. This contraption was then stuck to a microscope slide (using double sided tape)
484 for imaging on an upright microscope. This last step may be unnecessary depending on the
485 microscope stage and orientation.
486 Live imaging was performed on an upright Zeiss SP8 confocal microscope equipped
487 with Hybrid detectors in the Biocentre Imaging facility (University of Cologne). Image stacks
488 of 15-50 focal planes with z-steps ranging from 2-10 µm were taken with a 10x/0.3NA dry
489 objective or a 20×/0.7NA multi-immersion objective at intervals of 5-45 minutes. The
490 temperature of the sample during imaging could not be carefully regulated, but was typically

491 between 25-28 degrees. While this lack of temperature control is not ideal, it does not affect
492 the findings presented in this manuscript.
493 Photoconversion of NLS-tdEos protein was performed by constantly scanning the
494 region of interest for 20-30 seconds with the 405 wavelength laser at low power (5%). These
495 settings were manually determined on the above microscope, and need to be determined
496 independently on different systems. Photoconversions were performed during the final
497 uniform blastoderm stage, as photoconversion prior to this resulted in substantial diffusion
498 of the photoconverted protein during nuclei division. The positions of the different regions
499 of the embryo (75% EL etc.) were determined by measuring the length of each embryo in the
500 LASX software and selecting the appropriate region. Photoconversions were performed on
501 all embryos on the coverslip before setting up the timelapse, which led to a 0.5-2 hour delay
502 between performing the photoconversion and beginning the timelapse. As such, the
503 positions of the photoconverted region at the first time point in the timelapses in this
504 manuscript do not reflect the original region of photoconversion.
505 Imaging of fixed material was performed on an upright Zeiss SP8 confocal, an upright
506 Zeiss SP5 confocal microscope and an inverted Zeiss SP5 confocal microscope. The
507 *Drosophila gooseberry* expression patterns were kindly provided by Erik Clark and acquired
508 as in (65). Images and timelapses were analysed using FIJI (66) and Photoshop CS5. Manual
509 cell tracking was performed on confocal hyperstacks with MTrackJ (67). The figures were
510 arranged and the schematics created using Inkscape.
511
512
513 **Acknowledgements**

514 I would like to thank E. Clark for many stimulating discussions, extensive feedback on the
515 manuscript, and for providing the *Drosophila* images. I thank M. Pechmann for providing the
516 *NLS-tdEos* construct and S. Roth for supporting me during this project. In addition, I thank M.
517 Akam, M. Pechmann and S. Roth for comments on the manuscript.
518
519

520 **References**

521 1. Grimaldi D, Engel M. Evolution of the Insects. Cambridge University Press; 2005.
522 2. Anderson DT. Embryology and Phylogeny in Annelids and Arthropod. Pergamon Press;
523 1973.
524 3. Jaeger J. The gap gene network. Cell Mol Life Sci [Internet]. 2011 Jan [cited 2013 Mar
525 8];68(2):243–74. Available from:
526 http://www.pubmedcentral.nih.gov/articlerender.fcgi?artid=3016493&tool=pmcentr
527 ez&rendertype=abstract
528 4. Davis GK, Patel NH. SHORT, LONG, AND BEYOND: Molecular and Embryological
529 Approaches to. Annu Rev Entomol. 2002;(47):669–99.
530 5. Peel AD, Chipman AD, Akam M. Arthropod segmentation: beyond the Drosophila
531 paradigm. Nat Rev Genet [Internet]. 2005 Dec [cited 2010 Jul 6];6(12):905–16.
532 Available from: http://www.ncbi.nlm.nih.gov/pubmed/16341071
533 6. Choe CP, Miller SC, Brown SJ. A pair-rule gene circuit defines segments sequentially in
534 the short-germ insect Tribolium castaneum. Proc Natl Acad Sci U S A [Internet]. 2006
535 Apr 25;103(17):6560–4. Available from:
536 http://www.pubmedcentral.nih.gov/articlerender.fcgi?artid=1564201&tool=pmcentr
537 ez&rendertype=abstract

538 7. Sarrazin AF, Peel AD, Averof M. A segmentation clock with two-segment periodicity in
539 insects. Science [Internet]. 2012 Apr 20 [cited 2012 Oct 5];336(6079):338–41.
540 Available from: http://www.ncbi.nlm.nih.gov/pubmed/22403177
541 8. Clark E. Dynamic patterning by the Drosophila pair-rule network reconciles long-germ
542 and short-germ segmentation. PLOS Biol [Internet]. 2017 Sep 27;15(9):e2002439.
543 Available from: https://doi.org/10.1371/journal.pbio.2002439
544 9. Clark E, Peel AD. Evidence for the temporal regulation of insect segmentation by a
545 conserved set of developmental transcription factors. bioRxiv [Internet]. 2017 Jan 1;
546 Available from: http://biorxiv.org/content/early/2017/06/02/145151.abstract
547 10. Zhu X, Rudolf H, Healey L, François P, Brown SJ, Klingler M, et al. Speed regulation of
548 genetic cascades allows for evolvability in the body plan specification of insects. Proc
549 Natl Acad Sci [Internet]. 2017 Oct 10;114(41):E8646–55. Available from:
550 http://www.pnas.org/content/114/41/E8646.abstract
551 11. Irvine KD, Wieschaus E. Cell intercalation during Drosophila germband extension and
552 its regulation by pair-rule segmentation genes. Development [Internet]. 1994
553 Apr;120(4):827–41. Available from: http://www.ncbi.nlm.nih.gov/pubmed/7600960
554 12. Bertet C, Sulak L, Lecuit T. Myosin-dependent junction remodelling controls planar cell
555 intercalation and axis elongation. Nature [Internet]. 2004 Jun 10;429(6992):667–71.
556 Available from: http://dx.doi.org/10.1038/nature02590
557 13. Collinet C, Rauzi M, Lenne P, Lecuit T. Local and tissue-scale forces drive oriented
558 junction growth during tissue extension. Nat Cell Biol [Internet]. 2015 Sep
559 21;17(10):1247–58. Available from:
560 http://www.nature.com/doifinder/10.1038/ncb3226
561 14. Butler LC, Blanchard GB, Kabla AJ, Lawrence NJ, Welchman DP, Mahadevan L, et al.

562 Cell shape changes indicate a role for extrinsic tensile forces in Drosophila germ-band
563 extension. Nat Cell Biol. 2009 Jul;11(7):859–64.
564 15. Firmino AAP, Fonseca FC de A, de Macedo LLP, Coelho RR, Antonino de Souza Jr JD,
565 Togawa RC, et al. Transcriptome Analysis in Cotton Boll Weevil (Anthonomus grandis)
566 and RNA Interference in Insect Pests. PLoS One [Internet]. 2013;8(12):e85079.
567 Available from: http://dx.plos.org/10.1371/journal.pone.0085079
568 16. da Silva SM, Vincent J-P. Oriented cell divisions in the extending germband of
569 Drosophila Development [Internet]. 2007 Sep 1;134(17):3049
570 LP-3054. Available from: http://dev.biologists.org/content/134/17/3049.abstract
571 17. Liu PZ, Kaufman TC. Short and long germ segmentation: unanswered questions in the
572 evolution of a developmental mode. Evol Dev [Internet]. 2005;7(6):629–46. Available
573 from: http://www.ncbi.nlm.nih.gov/pubmed/16336416
574 18. Benton MA, Akam M, Pavlopoulos A. Cell and tissue dynamics during Tribolium
575 embryogenesis revealed by versatile fluorescence labeling approaches. Development
576 [Internet]. 2013 Jul 16 [cited 2013 Jul 16];140(15):3210–20. Available from:
577 http://dev.biologists.org/cgi/doi/10.1242/dev.096271
578 19. Nakamoto A, Hester SD, Constantinou SJ, Blaine WG, Tewksbury AB, Matei MT, et al.
579 Changing cell behaviours during beetle embryogenesis correlates with slowing of
580 segmentation. Nat Commun [Internet]. 2015;6:6635. Available from:
581 http://www.nature.com.libproxy.helsinki.fi/ncomms/2015/150410/ncomms7635/full
582 /ncomms7635.html
583 20. Paré AC, Vichas A, Fincher CT, Mirman Z, Farrell DL, Mainieri A, et al. A positional Toll
584 receptor code directs convergent extension in Drosophila. Nature [Internet]. 2014 Nov
585 2;515(7528):523–7. Available from: http://www.ncbi.nlm.nih.gov/pubmed/25363762

586 21. Benton MAA, Pechmann M, Frey N, Stappert D, Conrads KHKH, Chen Y-TY-T, et al. Toll
587 Genes Have an Ancestral Role in Axis Elongation. Curr Biol [Internet].
588 2016;26(12):1609–15. Available from:
589 http://linkinghub.elsevier.com/retrieve/pii/S0960982216304092
590 22. Campos-Ortega J a, Hartenstein V. The embryonic development of Drosophila
591 melanogaster. 2nd ed. Springer-Verlag Berlin Heidelberg; 1997.
592 23. Schönauer A, Paese CLB, Hilbrant M, Leite DJ, Schwager EE, Feitosa NM, et al. The Wnt
593 and Delta-Notch signalling pathways interact to direct pair-rule gene expression via
594 caudal during segment addition in the spider Parasteatoda tepidariorum.
595 Development [Internet]. 2016;2455–63. Available from:
596 http://dev.biologists.org/content/early/2016/06/09/dev.131656.abstract
597 24. Janssen R. Gene expression suggests double-segmental and single-segmental
598 patterning mechanisms during posterior segment addition in the beetle Tribolium
599 castaneum. Int J Dev Biol. 2014;58(5).
600 25. van der Zee M, Berns N, Roth S. Distinct Functions of the Tribolium zerknullt Genes in
601 Serosa Specification and Dorsal Closure. Curr Biol. 2005;15:624–36.
602 26. Falciani F, Hausdorf B, Schröder R, Akam M, Tautz D, Denell R, et al. Class 3 Hox genes
603 in insects and the origin of zen. Proc Natl Acad Sci USA. 1996;93:8479–84.
604 27. Handel K, Grünfelder CG, Roth S, Sander K. Tribolium embryogenesis: a SEM study of
605 cell shapes and movements from blastoderm to serosal closure. Dev Genes. 2000;
606 28. Nunes da Fonseca R, von Levetzow C, Kalscheuer P, Basal A, van der Zee M, Roth S.
607 Self-Regulatory Circuits in Dorsoventral Axis Formation of the Short-Germ Beetle
608 Tribolium castaneum. Dev Cell [Internet]. 2008;14(4):605–15. Available from:
609 http://www.sciencedirect.com/science/article/pii/S1534580708001056

610 29. Schmidt-Ott U, Kwan CW. Morphogenetic functions of extraembryonic membranes in
611 insects. Curr Opin Insect Sci [Internet]. 2016;13:86–92. Available from:
612 http://dx.doi.org/10.1016/j.cois.2016.01.009
613 30. Panfilio K a. Extraembryonic development in insects and the acrobatics of
614 blastokinesis. Dev Biol [Internet]. 2008 Jan [cited 2011 Mar 10];313(2):471–91.
615 Available from: http://www.ncbi.nlm.nih.gov/pubmed/18082679
616 31. Benton MAA, Pavlopoulos A. Tribolium embryo morphogenesis: May the force be with
617 you. Bioarchitecture. 2014;4(1):16–21.
618 32. Jacobs CGC, Spaink HP, van der Zee M. The extraembryonic serosa is a frontier
619 epithelium providing the insect egg with a full-range innate immune response. Elife
620 [Internet]. 2014;3:1–21. Available from:
621 http://elifesciences.org/lookup/doi/10.7554/eLife.04111
622 33. Jacobs CGC, Van Der Zee M. Immune competence in insect eggs depends on the
623 extraembryonic serosa. Dev Comp Immunol. 2013;41(2).
624 34. Lynch JA, Roth S. The evolution of dorsal-ventral patterning mechanisms in insects.
625 Genes Dev [Internet]. 2011 Jan 15 [cited 2011 Jan 18];25(2):107–18. Available from:
626 http://www.pubmedcentral.nih.gov/articlerender.fcgi?artid=3022256&tool=pmcentr
627 ez&rendertype=abstract
628 35. Horn T, Panfilio KA. Novel functions for Dorsocross in epithelial morphogenesis in the
629 beetle Tribolium castaneum. Development [Internet]. 2016;143(16):3002–11.
630 Available from: http://dev.biologists.org/lookup/doi/10.1242/dev.133280
631 36. Anderson DT. The Development of Holometabolous Insects. In: Counce SJ, Waddinton
632 CH, editors. Developmental systems Insects, Vol 1. New York: Academic Press; 1972.
633 p. 165–242.

634 37. Anderson DT. The Development of Hemimetabolous Insects. In: Counce SJ,
635 Waddington CH, editors. Developmental systems Insects, Vol 1. New York: Academic
636 Press; 1972. p. 95–163.
637 38. Aranda M, Marques-Souza H, Bayer T, Tautz D. The role of the segmentation gene
638 hairy in Tribolium. Dev Genes Evol [Internet]. 2008 Sep [cited 2013 Mar
639 11];218(9):465–77. Available from:
640 http://www.pubmedcentral.nih.gov/articlerender.fcgi?artid=2522291&tool=pmcentr
641 ez&rendertype=abstract
642 39. Schulz C, Schröder R, Hausdorf B, Wolff C, Tautz D. A caudal homologue in the short
643 germ band beetle Tribolium shows similarities to both, the Drosophila and the
644 vertebrate caudal expression patterns. Dev Genes Evol [Internet]. 1998 [cited 2012
645 Jan 20];208(5):283–9. Available from:
646 http://www.springerlink.com/index/u6epmj98hxfr9jmd.pdf
647 40. Mlodzik M, Gehring WJ. Expression of the caudal gene in the germ line of Drosophila:
648 Formation of an RNA and protein gradient during early embryogenesis. Cell [Internet].
649 1987;48(3):465–78. Available from:
650 http://www.sciencedirect.com/science/article/pii/0092867487901978
651 41. Tomancak P, Berman BP, Beaton A, Weiszmann R, Kwan E, Hartenstein V, et al. Global
652 analysis of patterns of gene expression during Drosophila embryogenesis. Genome
653 Biol. 2007;8(7):R145.
654 42. Hammonds AS, Bristow CA, Fisher WW, Weiszmann R, Wu S, Hartenstein V, et al.
655 Spatial expression of transcription factors in Drosophila embryonic organ
656 development. Genome Biol. 2013 Dec;14(12):R140.
657 43. Tomancak P, Beaton A, Weiszmann R, Kwan E, Shu S, Lewis SE, et al. Systematic

658 determination of patterns of gene expression during Drosophila embryogenesis.
659 Genome Biol. 2002;3(12):RESEARCH0088.
660 44. Sam S, Leise W, Hoshizaki DK. The serpent gene is necessary for progression through
661 the early stages of fat-body development. Mech Dev [Internet]. 1996 Dec;60(2):197–
662 205. Available from: http://www.ncbi.nlm.nih.gov/pubmed/9025072
663 45. Sachs L, Chen YT, Drechsler A, Lynch JA, Panfilio KA, Lässig M, et al. Dynamic BMP
664 signaling polarized by Toll patterns the dorsoventral axis in a hemimetabolous insect.
665 Elife. 2015;4(MAY).
666 46. Handel K, Basal A, Fan X, Roth S. Tribolium castaneum twist: gastrulation and
667 mesoderm formation in a short-germ beetle. Dev Genes Evol. 2005;215:13–31.
668 47. van der Zee M, Stockhammer O, von Levetzow C, Nunes da Fonseca R, Roth S.
669 Sog/Chordin is required for ventral-to-dorsal Dpp/BMP transport and head formation
670 in a short germ insect. Proc Natl Acad Sci U S A [Internet]. 2006 Oct;103(44):16307–
671 12. Available from:
672 http://www.pubmedcentral.nih.gov/articlerender.fcgi?artid=1637578&tool=pmcentr
673 ez&rendertype=abstract
674 48. Stappert D, Frey N, von Levetzow C, Roth S. Genome-wide identification of Tribolium
675 dorsoventral patterning genes. Development [Internet]. 2016 Jul 1;143(13):2443–54.
676 Available from: http://dev.biologists.org/lookup/doi/10.1242/dev.130641
677 49. van der Zee M, Benton MAA, Vazquez-Faci T, Lamers GEMEM, Jacobs CGCGC,
678 Rabouille C. Innexin7a forms junctions that stabilize the basal membrane during
679 cellularization of the blastoderm in Tribolium castaneum. Development [Internet].
680 2015;142(12):2173–83. Available from:
681 http://dev.biologists.org/cgi/doi/10.1242/dev.097113

682 50. Rauzi M, Krzic U, Saunders TE, Krajnc M, Ziherl P, Hufnagel L, et al. Embryo-scale tissue
683 mechanics during Drosophila gastrulation movements. Nat Commun [Internet]. 2015
684 Oct 26;6:8677. Available from: http://dx.doi.org/10.1038/ncomms9677
685 51. Leptin M, Grunewald B. Cell shape changes during gastrulation in Drosophila.
686 Development [Internet]. 1990 Sep 1;110(1):73 LP-84. Available from:
687 http://dev.biologists.org/content/110/1/73.abstract
688 52. Roth S. Gastrulation in Other Insects. In: Stern CD, editor. Gastrulation From Cells to
689 Embryo. New York: Cold Spring Harbor Laboratory Press; 2004. p. 105–21.
690 53. Ewen-Campen B, Jones TEM, Extavour CG. Evidence against a germ plasm in the
691 milkweed bug Oncopeltus fasciatus, a hemimetabolous insect. Biol Open [Internet].
692 2013;2(6):556–68. Available from:
693 http://www.pubmedcentral.nih.gov/articlerender.fcgi?artid=3683158&tool=pmcentr
694 ez&rendertype=abstract
695 54. Erezyilmaz DF, Kelstrup HC, Riddiford LM. The nuclear receptor E75A has a novel pair-
696 rule-like function in patterning the milkweed bug, Oncopeltus fasciatus. Dev Biol
697 [Internet]. 2009 Oct 1 [cited 2013 May 1];334(1):300–10. Available from:
698 http://www.pubmedcentral.nih.gov/articlerender.fcgi?artid=2749522&tool=pmcentr
699 ez&rendertype=abstract
700 55. Liu PZ, Kaufman TC. even-skipped is not a pair-rule gene but has segmental and gap-
701 like functions in Oncopeltus fasciatus, an intermediate germband insect. Development
702 [Internet]. 2005 May [cited 2013 Mar 7];132(9):2081–92. Available from:
703 http://www.ncbi.nlm.nih.gov/pubmed/15788450
704 56. Peel AD. The evolution of developmental gene networks: lessons from comparative
705 studies on holometabolous insects. Philos Trans R Soc Lond B Biol Sci [Internet]. 2008

706 Apr 27 [cited 2012 Oct 9];363(1496):1539–47. Available from:
707 http://www.pubmedcentral.nih.gov/articlerender.fcgi?artid=2615820&tool=pmcentr
708 ez&rendertype=abstract
709 57. Turner FR, Mahowald AP. Scanning Electron Microscopy of Drosophila Embryogenesis
710 II. Gastrulation and Segmentation. 1977;416:403–16.
711 58. Oberhofer G, Grossmann D, Siemanowski JL, Beissbarth T, Bucher G. Wnt/beta-
712 catenin signaling integrates patterning and metabolism of the insect growth zone.
713 Development [Internet]. 2014 Dec;141(24):4740–50. Available from:
714 http://dev.biologists.org/cgi/doi/10.1242/dev.112797
715 59. Nagy LM, Carroll S. Conservation of wingless patterning functions in the short-germ
716 embryos of Tribolium castaneum. Nature [Internet]. 1994;367(6462):460–3. Available
717 from: http://biomednet.com/db/medline/94150623
718 60. Brown SJ, Patel NH, Denell RE. Embryonic expression of the single Tribolium engrailed
719 homolog. Dev Genet [Internet]. 1994;15(1):7–18. Available from:
720 http://dx.doi.org/10.1002/dvg.1020150103
721 61. Savard J, Marques-Souza H, Aranda M, Tautz D. A segmentation gene in tribolium
722 produces a polycistronic mRNA that codes for multiple conserved peptides. Cell
723 [Internet]. 2006 Aug 11 [cited 2013 May 1];126(3):559–69. Available from:
724 http://www.ncbi.nlm.nih.gov/pubmed/16901788
725 62. Carroll L. Alice's Adventures in Wonderland. New York: Macmillan; 1865.
726 63. Gillis WQ, Bowerman B a, Schneider SQ. The evolution of protostome GATA factors:
727 molecular phylogenetics, synteny, and intron/exon structure reveal orthologous
728 relationships. BMC Evol Biol [Internet]. 2008 Jan [cited 2012 Mar 4];8:112. Available
729 from:

730 http://www.pubmedcentral.nih.gov/articlerender.fcgi?artid=2383905&tool=pmcentr
731 ez&rendertype=abstract
732 64. Nagai T, Ibata K, Park ES, Kubota M, Mikoshiba K, Miyawaki A. A variant of yellow
733 fluorescent protein with fast and efficient maturation for cell-biological applications.
734 Nat Biotechnol [Internet]. 2002 Jan 1;20:87. Available from:
735 http://dx.doi.org/10.1038/nbt0102-87
736 65. Clark E, Akam M. Odd-paired controls frequency doubling in Drosophila segmentation
737 by altering the pair-rule gene regulatory network. Elife. 2016 Aug;5.
738 66. Schindelin J, Arganda-Carreras I, Frise E, Kaynig V, Longair M, Pietzsch T, et al. Fiji: an
739 open-source platform for biological-image analysis. Nat Methods [Internet]. 2012 Jul
740 [cited 2013 Mar 4];9(7):676–82. Available from:
741 http://www.ncbi.nlm.nih.gov/pubmed/22743772
742 67. Meijering E, Dzyubachyk O, Smal I. Methods for cell and particle tracking. [Internet].
743 1st ed. Vol. 504, Methods in enzymology. United States: Elsevier Inc.; 2012 [cited 2013
744 Mar 4]. 183-200 p. Available from: http://www.ncbi.nlm.nih.gov/pubmed/22264535
745
746
747 **Fig 1. Schematics of development in *Drosophila* and *Tribolium*.** The two left columns show
748 schematics of *Drosophila* embryos from the uniform blastoderm stage to the extended
749 germband stage. The right three columns show schematics of *Tribolium* embryos at
750 comparable stages. The schematics in the right-most column show dissected, flatmounted
751 embryos. Red arrows display cell/tissue movement. The question marks highlight two
752 regions where the tissue boundaries are unknown/undescribed. Several features have been
753 omitted, including the yolk, mesoderm gastrulation, anterior gut formation and appendage

754 formation. The *Drosophila* fatemap is based on data from (22) and the references therein.
755 Refer to text for additional details.
756
757 **Fig 2. Live cell tracking reveals contribution of 'amnion' cells to embryonic tissue.** (A-F)
758 Time series from fluorescent live imaging of a *Tribolium* embryo expressing H2B-venus. The
759 serosa nuclei located above the germband have been manually removed from these frames,
760 but left in the surrounding territory (arrowhead in (A+A')). (A'-C') show optical transverse
761 sections of the respective frame at the position shown by the dashed line (the surface of the
762 egg is to the left). In (A-C), all nuclei that lie in a region of the 'amnion territory' in (A) have
763 been tracked and differentially labelled depending on whether they become part of the
764 embryo (magenta; labels disappear when nuclei join the germband), become located at the
765 edge of the germband (yellow) or remain in the 'amnion territory' (cyan). In (D-F), a line of
766 nuclei that lie in the 'amnion territory' in (D) have been tracked and differentially labelled
767 depending on whether they become part of the embryo (coloured points; daughter cells are
768 labelled in same colour as parent) or remain in the 'amnion territory' (cyan; no division takes
769 place). Note that in panel (D), the orange spot is mostly hidden below the yellow spot
770 because the nuclei in that region are partially overlapping when viewed as projections. The
771 first frame of the timelapse was defined as timepoint 0. In (A-F), embryos are oriented based
772 on the AP/DV polarity of the egg with anterior to the left and dorsal to the top. (A-C) are
773 maximum intensity projections of one egg hemisphere. (D-F) are average intensity
774 projections of 46 microns to specifically show the germband. Scale bars are 50 µm.
775
776 **Fig 3. Differential cell labelling reveals widespread movement of cells from the dorsal**
777 **epithelium to the ventral epithelium.** (A-J) Time series from fluorescent live imaging of two

778 *Tribolium* embryos expressing NLS-tdEos showing unconverted protein (magenta) and
779 photoconverted protein (cyan). In (A-F') a patch of nuclei at the posterior-dorsal region of
780 the blastoderm were photoconverted. Panels (A-F) show the posterior region of the
781 germband during late GBE and panels (A'-F') show optical transverse sections made at the
782 position of the dashed line at each timepoint (roughly following the same nuclei). Serosa
783 nuclei are marked by white crosses in the transverse sections. In (G-J), a patch of nuclei at
784 the anterior-lateral region of the blastoderm were photoconverted. Panels (G-J) show the
785 anterior of the germband during condensation and GBE. In both embryos, all converted
786 nuclei are initially located in the dorsal epithelium, but most move into the ventral
787 epithelium during GBE. (K-L) Schematics showing the classic and revised models of the
788 *Tribolium* germband (presumptive amnion is shown in purple, presumptive embryo is shown
789 in grey, red arrows show the newly discovered tissue flow). The first frame of the timelapses
790 was defined as timepoint 0. In (A-J), embryos are oriented based on the AP/DV polarity of
791 the egg with anterior to the left and dorsal to the top. In (A'-F'), the surface of the egg is
792 oriented to the left. In (K-L), schematics show flatmounted germbands with the focus on the
793 dorsal epithelium, the anterior to the left and the orthogonal sections are oriented with the
794 dorsal half of the germand to the left. (A-J) are maximum intensity projections of one egg
795 hemisphere. Scale bars are 50 µm.
796
797 **Fig 4. Development of the putative amnion.** (A-A'') *Tribolium* embryo transiently expressing
798 the membrane marker GAP43-YFP. (A) shows an overview of the whole egg, (A') shows the
799 dorsal epithelium of the same embryo at the position of the white box, (A'') is an optical
800 sagittal section at the position of the dashed line in (A') showing the apical-basal height of
801 cells of the dorsal epithelium. (B) *Tc-srp* (red) expression in a flatmounted *Tribolium*

802 germband also showing nuclei (DAPI, blue). The strong *Tc-srp* signal in nuclei may suggest
803 nuclear or peri-nuclear localisation of the transcript, or it may be due to the cell body being
804 flattened. The strong patch of expression at the anterior medial region is from cells beneath
805 the ventral ectoderm (see Supplemental Fig 1 for a full expression series). (C-E) Extended
806 germband stage *Tribolium* embryos transiently expressing NLS-tdEos showing unconverted
807 protein (magenta) and photoconverted protein (cyan). In each embryo, the clone of
808 converted cells spans the entire amnion. (C_{1-2}) show both sides of the same embryo in which
809 a 6 nuclei wide patch of dorsal-most cells located at 50% EL were photoconverted at the
810 blastoderm stage. (E) shows an embryo in which a 3 nuclei wide patch of dorsal-most cells
811 located at 25% EL were photoconverted at the blastoderm stage. (F) shows an embryo in
812 which a 3 nuclei wide by 6 nuclei long patch of dorsal-most cells located at roughly 2-10% EL
813 were photoconverted at the blastoderm stage. In (A) and (C-E), embryos are oriented based
814 on the AP/DV polarity of the egg with anterior to the left and dorsal to the top. In (A''), the
815 surface of the egg is oriented to the bottom. In (B), the anterior of the germband is to the
816 left. (A) is an average intensity projection of one egg hemisphere. (A') is an average intensity
817 projection of 6 µm to specifically show the dorsal epithelium. (B) is a maximum intensity
818 projection of the whole germband. (C-E) are maximum intensity projections of one egg
819 hemisphere. Abbreviations are: ventral ectoderm (VE) and dorsal ectoderm (DE). Scale bars
820 are 50 µm.
821
822 **Fig 5. Schematics showing the classic and revised *Tribolium* fatemaps and germband**
823 **models.** Schematics drawn as in Fig 1 to show the classic fatemap and germband model and
824 the revised fatemap and model based on the results of this manuscript. Note that the
825 posterior amnion/embryo boundary is unclear. The schematics of the flatmounted

826 germbands are drawn with the focus on the dorsal epithelium. See text for additional details,
827 and Supplemental Fig 6 for an extended figure.
828
829 **Fig 6. Representation of the *Tribolium* germband as a cylinder.** (A_1) the germband of
830 *Tribolium* (and other insects) is usually drawn as it is in *in vivo*, that is, as a flattened shape
831 with the ventral cell fates to the top and the dorsal cell fates to the bottom. However, the
832 embryo can be unflattened (A_2) without changing the planar dimensions of the tissue itself,
833 and rotated (A_3) such that the dorsal-ventral axis is oriented in the widely accepted standard
834 of dorsal to the top and ventral to the bottom. When this is done, and third dimension is
835 incorporated to show the AP axis (A_4), the similarities in tissue boundaries and tissue
836 rearrangements in *Tribolium* and *Drosophila* (B) become obvious. Note that while both (A_4)
837 and (B) are cylindrical, the epithelium of the *Tribolium* germband inverts during embryo
838 condensation so the apical surface of the embryo faces inwards. Both (A) and (B) are
839 sections from roughly the middle of the respective embryo during GBE. Possible flattening of
840 dorsal tissue in *Drosophila* has been omitted due to a lack of detailed data at this stage.
841
842 **Supplementary Figure 1. Results of photoconversions at 50% egg length.** NLS-tdEos labelled
843 extended germband stage *Tribolium* embryos in which a patch of blastoderm nuclei were
844 photoconverted at 50% egg length (from the posterior pole) at different DV positions. The
845 approximate DV position of the patch and the approximate DV width of the clone (in terms
846 of nuclei number) are shown. The dorsal labelled embryo is shown from both sides to
847 demonstrate the photoconverted nuclei cover the full DV extent of the amnion (arrows).
848 Unconverted protein is shown in magenta, converted protein is shown in cyan. Images are

849 maximum intensity projections of one egg hemisphere. All eggs are oriented with the
850 anterior to the left and ventral to the bottom. Scale bars are 100 µm.
851
852 **Supplementary Figure 2. Results of photoconversions at 25% egg length.** NLS-tdEos labelled
853 extended germband stage *Tribolium* embryos in which a patch of blastoderm nuclei were
854 photoconverted at 25% egg length (from the posterior pole) at different DV positions. The
855 approximate DV position of the patch and the approximate DV width of the clone (in terms
856 of nuclei number) are shown. Unconverted protein is shown in magenta, converted protein
857 is shown in cyan. Images are maximum intensity projections of one egg hemisphere. All eggs
858 are oriented with the anterior to the left and ventral to the bottom. Scale bars are 100 µm.
859
860 **Supplementary Figure 3. Results of photoconversions near the posterior pole.** NLS-tdEos
861 labelled extended germband stage *Tribolium* embryos in which a patch of blastoderm nuclei
862 were photoconverted near the posterior pole at different DV positions. The approximate DV
863 position of the patch and the approximate DV width of the clone (in terms of nuclei number)
864 are shown. The second dorsally labelled embryo is shown at high magnification at two
865 timepoints and with a transverse section (at the position of the dashed green line) to show
866 the movement of tissue from the dorsal epithelium into the hindgut. Unconverted protein is
867 shown in magenta, converted protein is shown in cyan. Images are maximum intensity
868 projections of one egg hemisphere except for the bottom three embryos, which are shown
869 as maximum intensity projects through the germband in order to better show the labelled
870 nuclei. All eggs are oriented with the anterior to the left and ventral to the bottom except
871 for the second timepoint of the second dorsal view, which is shown with the posterior of the
872 germband to the left. Scale bars are 100 µm.

873

874 **Supplementary Figure 4. *Tc-cad* is expressed further to the anterior in the dorsal**

875 **epithelium than in the ventral epithelium.** (A-A'') show maximum intensity projections of

876 the posterior region of a flatmounted *Tribolium* germband shortly after serosa window

877 closure stained to show nuclei (DAPI, blue) and the mRNA expression pattern of *Tc-cad* (red).

878 The panels beside or below each main panel show optical sections through the germband at

879 the position of the respective coloured line in the main panel. (B-B'') show maximum

880 intensity projections of approximately one half of the germband from the lateral side (i.e.

881 projections of optical sagittal sections from the midline to the lateral edge of the germband).

882 Scale bar is 100 µm.

883

884 **Supplementary Figure 5. RNA expression of the *Tribolium* ortholog of the GATA factor**

885 ***serpent.*** (A-F) whole mount and (G-J) flatmount *Tribolium* embryos from the pre-blastoderm

886 to the retracting germband stage stained for *Tc-srp* mRNA (red) and nuclei (DAPI, blue). (G_1)

887 and (G_2) show the same embryo imaged from both sides. (H_1) and (H_2) show projections

888 from the dorsal epithelium (H_1) and the ventral epithelium (H_2) of the same embryo. *Tc-srp*

889 mRNA is maternally provided (A), and expression is ubiquitous until the late blastoderm

890 stage (B-C) when expression clears from the blastoderm but persists in the yolk nuclei

891 (scattered spots in (D-E)). During embryo condensation, *de novo* expression arises in a patch

892 of blastoderm cells at the anterior medial region (arrowhead in F). This patch of *Tc-srp*

893 expressing cells invaginates as part of the ventral furrow and becomes located beneath the

894 ectoderm (arrowhead in G_1-H_3). This expression domain is likely homologous to the anterior

895 ventral expression domain in *Drosophila* that marks the prohemocytes. During serosa

896 window closure, expression appears in a ring of dorsal epithelium cells (G_1). After serosa

897 window closure, expression persists in the dorsal epithelium (H_1) and (H_3). Unlike *Drosophila*,
898 there is no expression domain at the posterior of the blastoderm (E) or the early germband
899 (G_2). After germband elongation, a *de novo* expression domain appears at the posterior most
900 point of the embryo (I_1). Given the location of this domain at the base of the forming
901 hindgut, this is likely the posterior endoderm primordium. Expression can also be seen in a
902 patch of amnion that has remained attached to the germband (arrow in I_2), but most of the
903 rest of the amnion has been lost. Several other regions of expression can be seen, including
904 in the presumptive fat body (the segmental domains running down the body), in
905 presumptive hemocyte clusters (the two side-by-side domains in the anterior), and in an
906 anterior domain that may mark the anterior endoderm primordium. Expression also persists
907 in the yolk nuclei (data not shown). All embryos are shown with anterior to the left. (E-E'') is
908 oriented with the ventral to the bottom, (F-F'') is oriented as a ventral view. (H_3-H_3'') is an
909 optical sagittal section at approximately the midline of the embryo in (H_2). (A-F) are
910 maximum intensity projections of one egg hemisphere. (G_1-G_2''), (I1-I1'') and (J-J'') are
911 maximum intensity projections of flatmounted germbands. (I_2-I_2'') is a maximum intensity
912 projection of part of the germband to better show the amnion/dorsal epithelium. Scale bars
913 are 50 µm.
914
915 **Supplementary Figure 6. Extended schematics showing the classic and revised *Tribolium***
916 **fatemaps and germband models.** Refer to Fig 5 and the text for details.
917
918 **Supplementary Figure 7. Tissue specific cell shape changes during *Tribolium* condensation**.
919 Stills from timelapses of two *Tribolium* embryos transiently expressing GAP43YFP to label
920 membranes. The second panel of each timepoint shows optical transverse sections at the

921 position of the dashed line in the related panel. Ventral and lateral ectoderm becomes
922 columnar, while dorsal ectoderm becomes flattened. The non-columnar cells at the bottom
923 of the left hand embryo are likely the presumptive mesoderm. The first frame of the
924 timelapses was defined as timepoint 0. Both embryos are oriented with the anterior to the
925 left and ventral to the bottom. Abbreviations are: Dorsal (Dor), Lateral (Lat), Ventral (Ven)
926 and Ectoderm (Ect). Scale bars are 100 µm.
927
928 **Supplementary Figure 8. DV dynamics of the segment polarity gene *gooseberry* in**
929 ***Drosophila*.** Whole mount *Drosophila* embryos from the blastoderm stage (late stage 5) until
930 the extending germband stage (late stage 7/early stage 8). The red arrows in the 2nd and 3rd
931 panels highlight the dorsal-to-ventral tissue flow and the GBE. The vertical arrow is at
932 parasegment boundary 8/9, and is the same size in both panels. All embryos are
933 ventrolateral views with anterior to the left and dorsal to the top. Scale bar is 100 µm.
934 Images were kindly provided by Erik Clark.
935
936
937 **Supplementary Movie 1.** Confocal timelapse of a *Tribolium* embryo transiently expressing
938 H2B-ven to mark nuclei. A maximum intensity projection of one egg hemisphere is shown.
939 Anterior is to the left, the ventral side of the egg is to the bottom.
940
941 **Supplementary Movie 2.** Same timelapse as Supplementary Movie 1, but with nuclei of the
942 dorsal epithelium tracked until they join the ventral epithelium. Nuclei that join the ventral
943 epithelium are labelled magenta, nuclei that become located at the edge of the germband
944 are labelled yellow, nuclei that remain in the dorsal epithelium are labelled cyan. Anterior is

945 to the left, the ventral side of the egg is to the bottom. See Fig 2(A-C) for more details.

946

947 **Supplementary Movie 3.** Same timelapse as Supplementary Movie 1, but with a line of
948 nuclei of the dorsal epithelium tracked. Nuclei that remain in the dorsal epithelium are
949 labelled cyan. Anterior is to the left, the ventral side of the egg is to the bottom. See Fig 2(D-
950 F) for more details.

951

952 **Supplementary Movie 4.** Confocal timelapse of a *Tribolium* embryo transiently expressing
953 NLS-tdEos (magenta) with a line of blastoderm cells photoconverted (cyan). The brightness
954 increases approximately halfway through the movie due to a manual increase in laser power
955 at this point. A maximum intensity projection of one egg hemisphere is shown. Anterior is to
956 the left, the ventral side of the egg is to the bottom.

957

958 **Supplementary Movie 5.** Confocal timelapse of a *Tribolium* embryo transiently expressing
959 NLS-tdEos (magenta) with a patch of blastoderm cells photoconverted (cyan). (A) shows a
960 maximum intensity projection of one egg hemisphere is shown. (B) shows an optical
961 transverse section. (C) shows an average intensity projection of 10 optical transverse
962 sections. Anterior is to the left, the ventral side of the egg is to the bottom. See Fig 3(A-F) for
963 more details.

964

965 **Supplementary Movie 6.** Confocal timelapse of a *Tribolium* embryo transiently expressing
966 NLS-tdEos (magenta) with a patch of blastoderm cells photoconverted (cyan). Towards the
967 end of the timelapse, the cyan nuclei in the dorsal epithelium appear to condense
968 posteriorly to the hindgut. A maximum intensity projection of one egg hemisphere is shown.

969 Anterior is to the left, the ventral side of the egg is to the bottom.

970

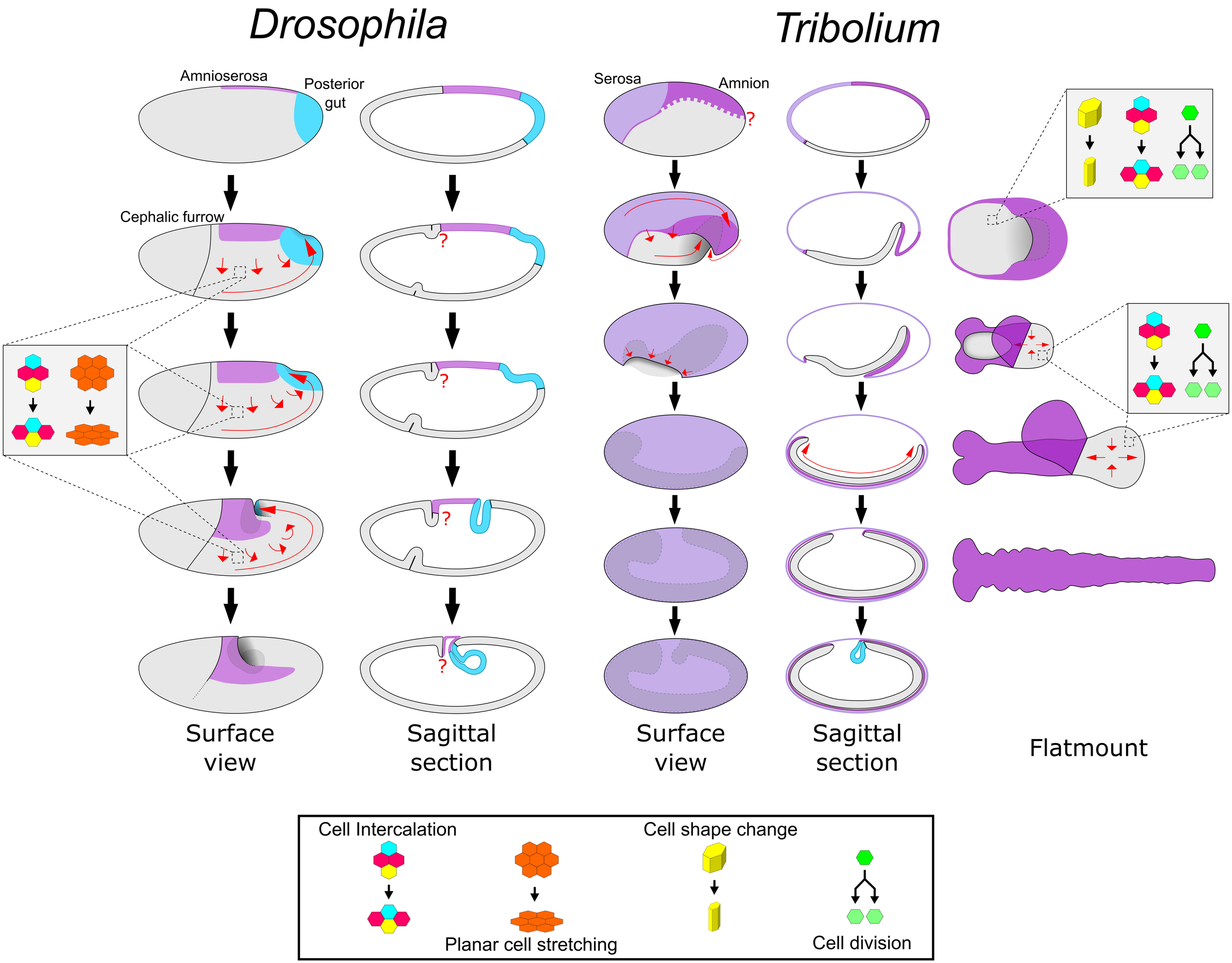
Drosophila
Tribolium
Amnioserosa
Posterior gut
Cephalic furrow
Serosa
Amnion
?
Surface view
Sagittal section
Surface view
Sagittal section
Flatmount
Cell Intercalation
Planar cell stretching
Cell shape change
Cell division

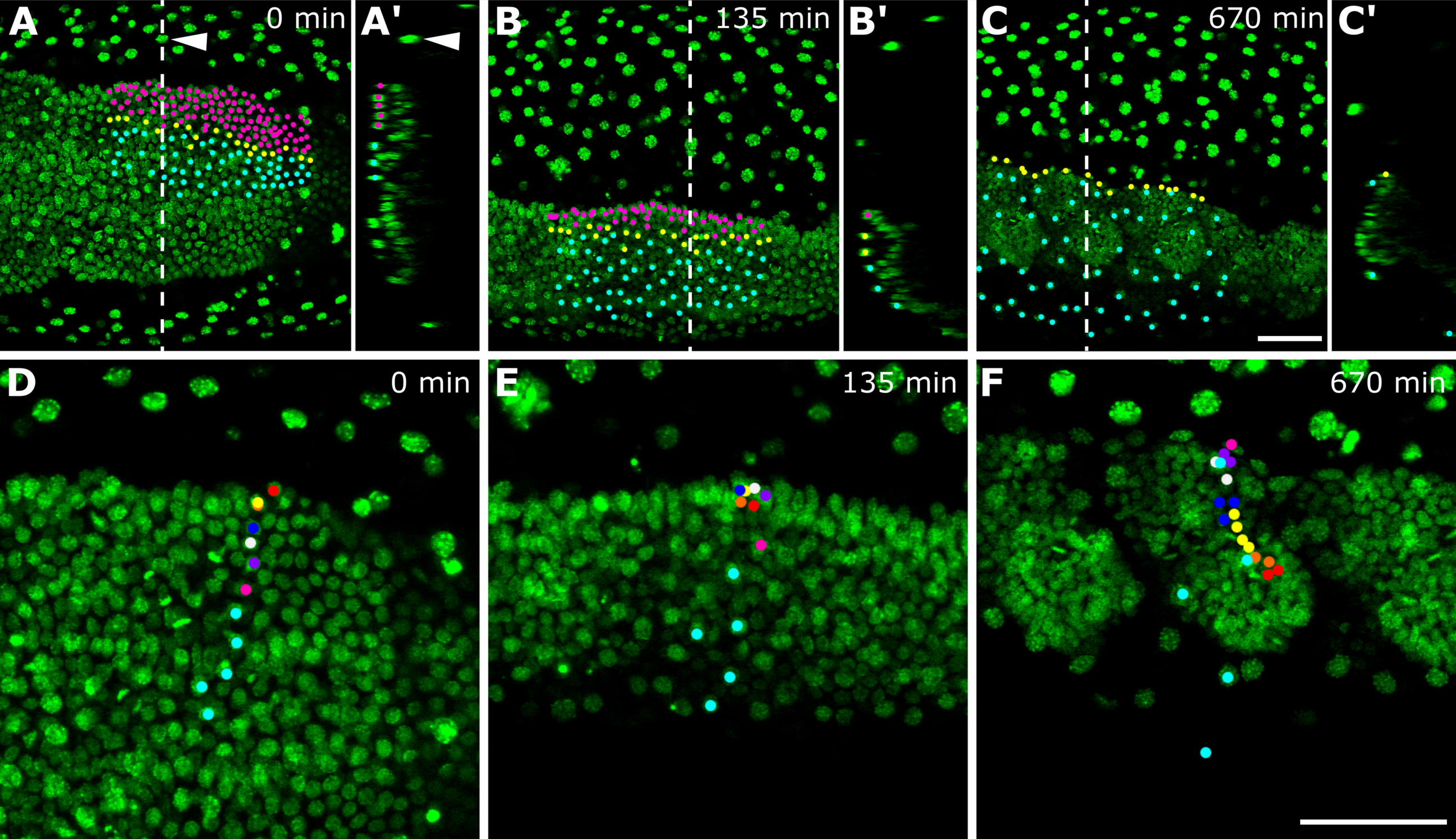
A
0 min
A'
B
135 min
B'
C
670 min
C'
D
0 min
E
135 min
F
670 min

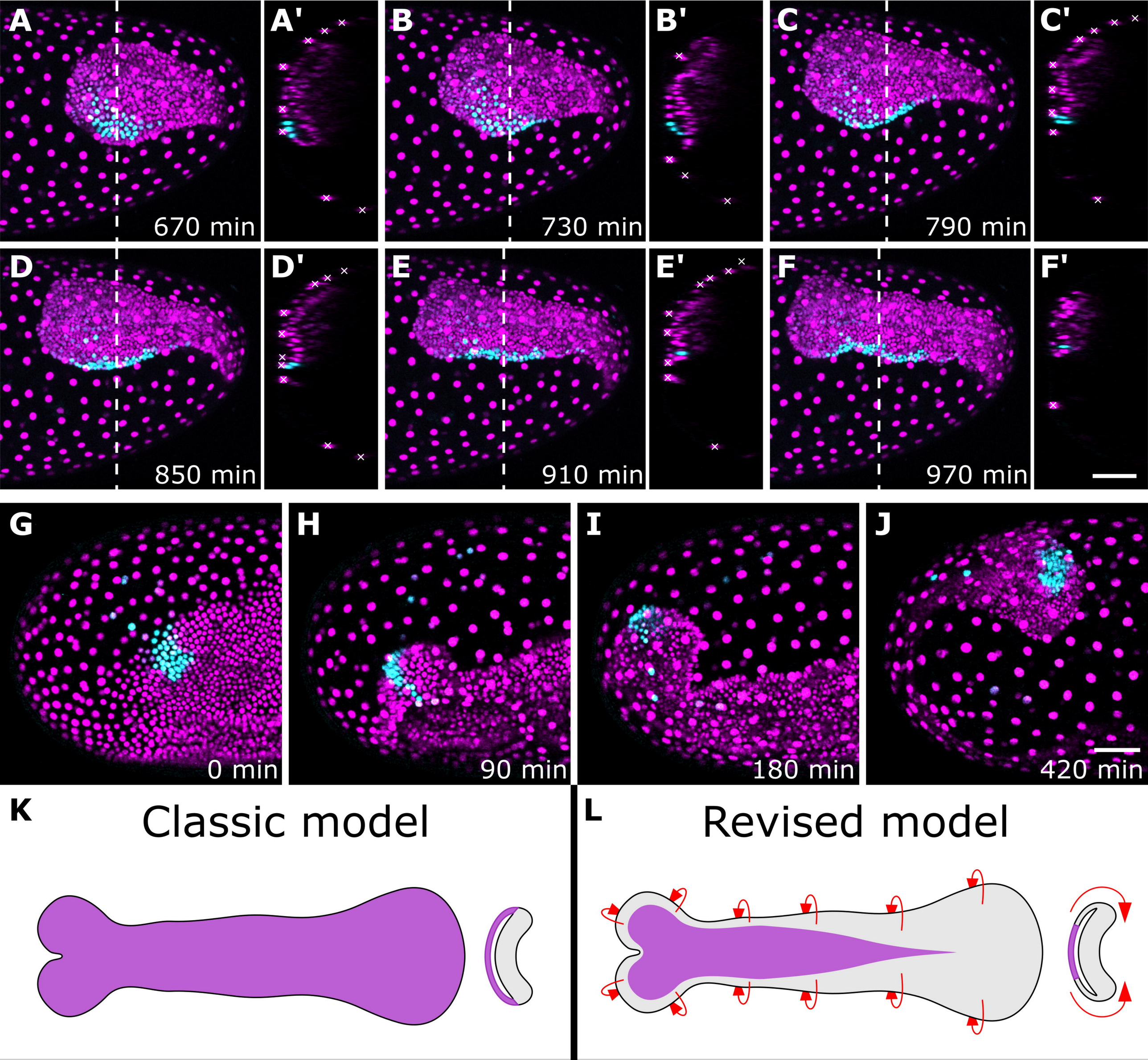
A
670 min
A'
B
730 min
B'
C
790 min
C'
D
850 min
D'
E
910 min
E'
F
970 min
F'
G
0 min
H
90 min
I
180 min
J
420 min
K
Classic model
L
Revised model

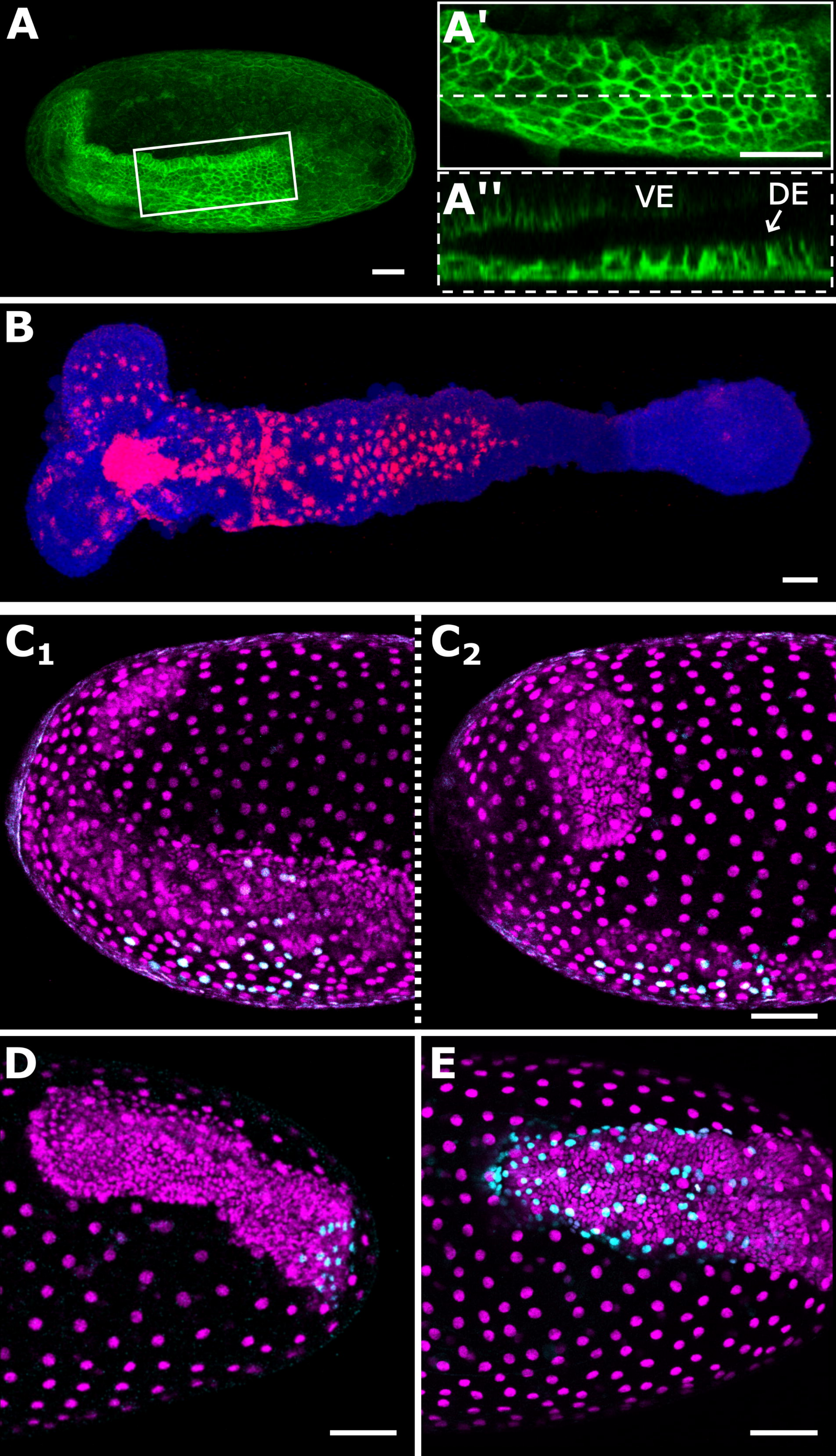
A
A'
A''
VE
DE
B
C1
C2
D
E

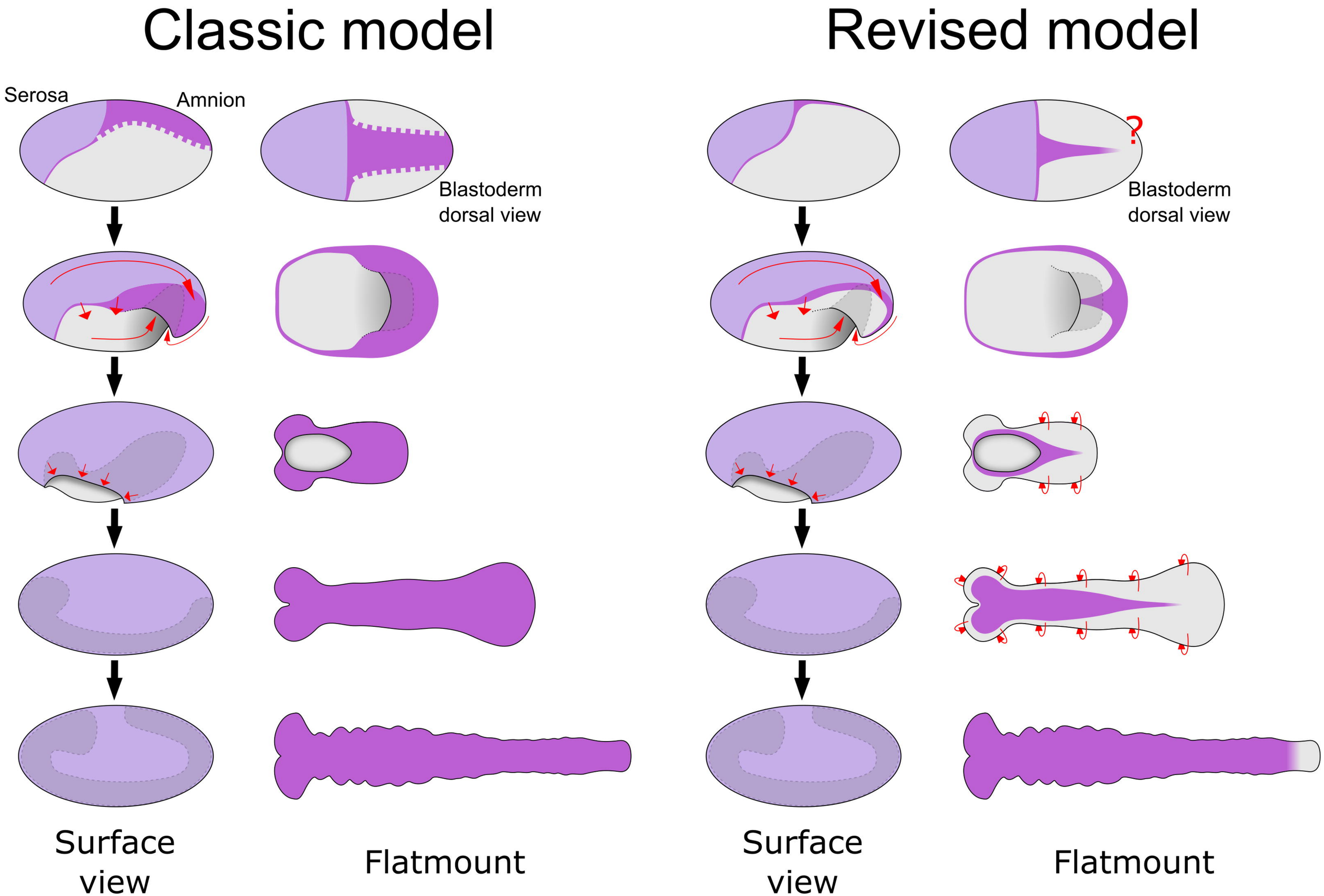
Classic model
Revised model
Serosa
Amnion
Blastoderm
dorsal view
?
Blastoderm
dorsal view
Surface
view
Flatmount
Surface
view
Flatmount

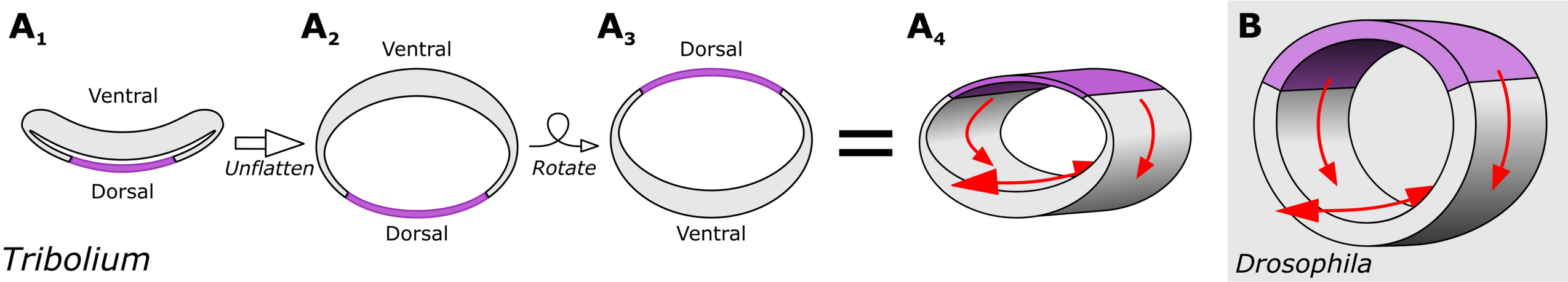
A1
Ventral
Dorsal
Unflatten
A2
Ventral
Dorsal
Rotate
A3
Dorsal
Ventral
A4
Tribolium
B
Drosophila